Intensity Measure Correlations Observed in the NGA-West2 Database, and Dependence of Correlations on Rupture and Site Parameters

Jack W. Baker,[a] **M.EERI, and Brendon A. Bradley,**[b] **M.EERI**

This manuscript reports ground motion intensity measure (*IM*) correlations for a number of *IM* types, as measured from the NGA-West2 database. *IM*s considered are Spectral Accelerations with periods from 0.01 s to 10 s, Peak Ground Acceleration, Peak Ground Velocity, and Significant Duration (for 5–75% and 5–95% definitions). Results are shown for correlations of both maximum-direction and geometric mean spectral acceleration values, given the need for such maximum-direction correlations in a new ASCE 7-16 procedure. Additionally, the potential magnitude-, distance- and site-condition-dependence of *IM* correlations are evaluated. The results are practically important as *IM* correlations are increasingly used in a range of engineering and seismic hazard calculations. We find that maximum-direction spectral correlations are comparable to correlations for other spectral acceleration definitions, and that the correlations have no practically significant dependence on magnitude, distance or site conditions. These results support the collective understanding that *IM* correlations are stable across a range of conditions, and as a result, that existing correlation models are generally appropriate for continued use in engineering calculations. [DOI: 10.1193/060716EQS095M]

INTRODUCTION

Many earthquake engineering calculations require probabilistic descriptions of ground shaking amplitude. When shaking amplitude is characterized by a single intensity measure (*IM*), this probabilistic description is usually obtained from a ground motion model (GMM) (e.g., Chiou and Youngs 2014), which provides the mean and standard deviation of the logarithm of the *IM*, conditional on rupture parameters such as magnitude and source-to-site distance (which we will denote here collectively as *Rup*) and site conditions (denoted *Site*).

When shaking intensity is characterized by multiple *IM*s, it is necessary to also quantify various correlation coefficients between the *IM*s, conditional on *Rup* and *Site*; specifically, multiple *IM*s are often well-represented by a lognormal distribution, in which case correlation coefficients for pairs of ln *IM* values provides a complete probabilistic description (e.g., Baker and Cornell 2005, Bradley 2010, Carlton and Abrahamson 2014). These correlation coefficients can be estimated from observed ground motion data, as will be discussed

[a] Department of Civil and Environmental Engineering, Stanford University, Stanford, CA 94305
[b] Department of Civil and Natural Resources Engineering, University of Canterbury, Christchurch, New Zealand

Earthquake Spectra, Volume 33, No. 1, pages 145–156, February 2017;

below, and there are a number of published models that predict these correlation coefficients. Modern GMMs for spectral acceleration (*SA*) values now sometimes provide these correlations (e.g., Abrahamson et al. 2014, Campbell and Bozorgnia 2014), but there are a number of other *IM*s for which pairwise correlations have been developed independently.

SA is an *IM* for which correlation models are frequently used. There are a number of ways, however, to compute "spectral acceleration" for a multi-component ground motion. The GMMs associated with the NGA-West2 project compute the median spectral acceleration at a given period observed over all horizontal orientations, while the ASCE 7 standard now considers maximum spectral acceleration observed over all horizontal orientations in both hazard analysis and response history analysis (ASCE 2016, Zimmerman et al. 2017). As the median amplitude is the 50th percentile and the maximum amplitude is the 100th percentile, these spectral acceleration definitions are denoted SA_{RotD50} and $SA_{RotD100}$, respectively (Boore 2010).

This paper presents an update and aggregated evaluation of models for the correlation of *IM*s, conditional on a rupture event, using the expanded ground motion database from the NGA-West2 project (Ancheta et al. 2014). Three primary results are presented in this paper. First, correlations from this dataset are compared with prior models developed from other data. Second, correlations for the $SA_{RotD100}$ definition of ground motion intensity are evaluated, as they have not previously been studied. Third, the dependence of correlations on rupture parameters such as earthquake magnitude and distance are studied, as the wider range of rupture scenarios in the NGA-West2 database enables an examination of the typical assumption that correlations are independent of such causal parameters.

DATA AND PROCESSING

Ground motion data from the NGA-West2 project ground motion database is used in this study (Ancheta et al. 2014). This database contains 21,539 ground motion recordings from shallow crustal earthquakes, with data coverage from $3 \leq M \leq 7.9$ and distances from $0 \leq R < 500$ km. To select usable data, only ground motions matching the selection criteria of Chiou and Youngs (2014) were used, including the restriction on usable frequencies.

For each *IM* of interest, within- and between-event residuals were computed using the following mixed effects formulation (Al Atik et al. 2010):

$$\ln im_{ij} = \mu_{\ln IM}(Rup_{ij}, Site_j) + dB_i + dW_{ij} \tag{1}$$

where $\ln im_{ij}$ is the natural logarithm of the *IM* of interest from the observed ground motion; and $\mu_{\ln IM}(Rup_{ij}, Site_j)$ is the prediction (from a GMM) of the mean ln *IM* value, as a function of *Rup* parameters such as magnitude (M) and distance (R), and *Site* parameters such as time-averaged shear wave velocity over the top 30 m of the site (V_{S30}). The subscripts indicate the j^{th} ground motion from the i^{th} earthquake, dB_i is the between-event residual for the i^{th} earthquake, and dW_{ij} is the within-event residual for the j^{th} observation from the i^{th} earthquake. The GMM also specifies the standard deviations of dB_i and dW_{ij}, denoted τ and ϕ, respectively. The mixed effects regression approach described by Jayaram and Baker (2010) is used to estimate dB_i for each earthquake and dW_{ij} for each ground motion in the considered database.

For *SA*, peak ground acceleration (PGA) and peak ground velocity (PGV), the Chiou and Youngs (2014) ground motion model was used (with no directivity modifications, and with the modifier model of Shahi and Baker (2014) for $SA_{RotD100}$ predictions). For 5–75% and 5–95% significant durations, the Afshari and Stewart (2016) ground motion model was used.

Then, for each pair of *IM*s, ground motions with usable values of both *IM*s were selected and a correlation coefficient computed using the following equation (which can be derived by applying the definition of the correlation coefficient to Equation 1):

$$\rho_{IM_1,IM_2} = \frac{\rho_{dB_1,dB_2}\tau_1\tau_2 + \rho_{dW_1,dW_2}\phi_1\phi_2}{\sigma_1\sigma_2} \tag{2}$$

where τ_k, ϕ_k and $\sigma_k = \sqrt{\tau_k^2 + \phi_k^2}$ are the between-event, within-event and total standard deviations for IM_k (specified by the GMM), and ρ_{dB_1,dB_2} and ρ_{dW_1,dW_2} are the correlation coefficients estimated here from the between- and within-event residuals. We note that, as Equation 2 is obtained from the residuals of Equation 1, it is a correlation coefficient for IM_1 and IM_2, conditional on *Rup* and *Site*, but the conditioning notation is suppressed for brevity.

RESULTS

The following subsections show results from correlation calculations using the data and approach described above. Correlations are computed using Equation 2, and unless otherwise noted the correlations are computed using all allowable ground motions with $M > 5$ and $R < 100$ km; these restrictions are put in place to focus on the ground motions of most engineering interest, although later we will study the potential impact of such restrictions. Spectral acceleration correlations are shown for SA_{RotD50} values unless otherwise noted.

COMPARISON TO PRIOR DATA AND MODELS

The *SA* correlations computed in this study are compared to several similar recently published models in Figure 1. Al Atik (2011) reported tabulated correlation coefficients from subduction ground motions. Akkar et al. (2014) and Cimellaro (2013) provided correlations from European ground motions, while Goda and Atkinson (2009) utilized Japanese ground motions. Baker and Jayaram (2008) used the NGA-West1 database of shallow crustal earthquake ground motions, which is a subset of the database used here, though they used fewer restrictions when identifying ground motions for analysis from the database. Baker and Jayaram (2008), Cimellaro (2013) and Goda and Atkinson (2009) provide analytical functions for predicting these correlations, while Al Atik (2011) and Akkar et al. (2014) provide tables of correlation coefficients. There are a number of additional correlation models in the literature, but most other models are either older or use data sets very similar to those considered here.

Figure 2 shows correlations of the non-spectral-acceleration *IM*s with *SA*s at a range of periods. The only relevant prior models are from Bradley (2011a, 2011b, 2012), and those are also plotted; we note that these predictive models were calibrated from a database that somewhat duplicates, but is much smaller in size, than the data set considered here.

A few comments can be made about these results. First, the Cimellaro (2013) model in Figure 1 appears to have a numerical error, as the predictions are significantly different than

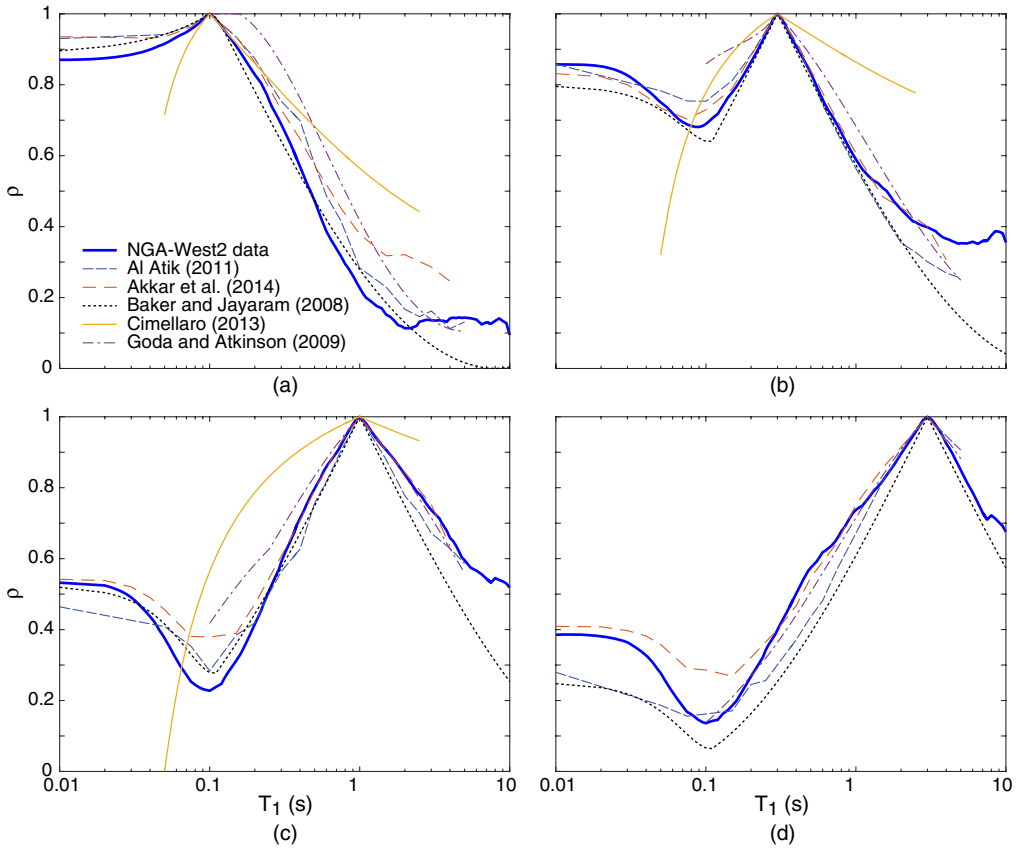

Figure 1. Correlation coefficients from the NGA-West2 data used in this study, compared to several other sources of correlation data. The x axis specifies one period, T_1, and the second period varies per sub-figure: (a) $T_2 = 0.1$ s, (b) $T_2 = 0.3$ s, (c) $T_2 = 1$ s, (d) $T_2 = 3$ s. Results are only plotted for period pairs where predictions were provided.

other models and data, and include unexpected features such as negative correlations for some period pairs.

Second, with the exception of Cimellaro, the models are generally in good agreement, with differences of less than 0.1 for most pairs of models and conditioning periods. This is striking, given the widely varying ground motion data used in these studies. Deviations among models exceed 0.1 for some short/long period *SA* pairs (e.g., $T_1 < 0.5$ s and $T_2 > 3$ s), *PGV* and $SA(0.1\,\text{s})$, and duration with long-period *SA*. These large-deviation cases typically have correlation coefficients between 0 and 0.5, and differences in these cases are less significant in terms of: (1) their effect on conditional distributions (as will be discussed further below), and (2) the standard error in the point estimate of the correlation is also larger for small ρ values.

Finally, we note that the duration correlations of Figure 2b are similar to the reference models for all *SA* periods. The negative correlations that occur at most periods are somewhat

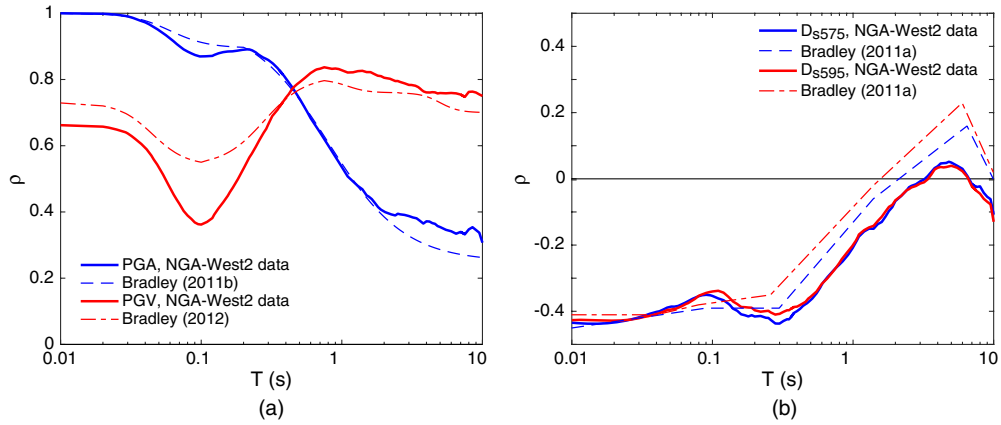

Figure 2. (a) Correlations of PGA and PGV with $SA(T)$, with the predictions of Bradley (2011b; 2012) superimposed for reference. (b) Correlations of significant duration with $SA(T)$, with the predictions of Bradley (2011a) superimposed for reference.

expected, as ground motions with longer-than-predicted durations tend to have ground motion energy arriving over a longer period of time, and thus less likely to cause large peak responses in a damped oscillator (while long-period oscillators require a longer duration of shaking to build up resonance and so have little or no negative correlation).

CORRELATIONS FOR MAXIMUM-DIRECTION RESPONSE SPECTRA

Figure 3 shows estimated *SA* correlations, as computed using Equation 2, for SA_{RotD50} and $SA_{RotD100}$ values observed in the database. Also shown for reference are correlation predictions from a reference model (Baker and Jayaram 2008). We see that the SA_{RotD50} and $SA_{RotD100}$ correlation coefficients are essentially identical. This result can be explained by noting that $SA_{RotD100}$ predictions use an equation that is essentially a linear transformation of Equation 1, and typical log standard deviations of SA_{RotD50} residuals are on the order of 0.65 to 0.8 (e.g., Chiou and Youngs 2014) while typical log standard deviations of $SA_{RotD100}/SA_{RotD50}$ ratios are less than 0.1 (e.g., Shahi and Baker 2014). This indicates that the $SA_{RotD100}$ values are quite similar to SA_{RotD50} values (in comparison to the similarity of observed and predicted SA_{RotD50} values), and thus correlations models for SA_{RotD50} can accurately be used as correlation models for $SA_{RotD100}$ values as well. Baker and Jayaram (2008) previously found that correlations for several other definitions of spectral acceleration (i.e., single component, geometric mean of two components, and a variant of the SA_{RotD50} definition) were also equivalent, so we see that spectral acceleration correlations are generally independent of the method used to define a ground motion's *SA*.

Note that these results quantify correlations in multi-directional shaking amplitude: there is no single orientation associated with the spectra or correlations. For example, a $SA_{RotD100}$ correlation coefficient indicates correlation of $SA_{RotD100}$ at one period with $SA_{RotD100}$ at some other period, though the orientations of the maximum-amplitude spectra at those two periods likely differ. There is also no single orientation associated with SA_{RotD50} correlations.

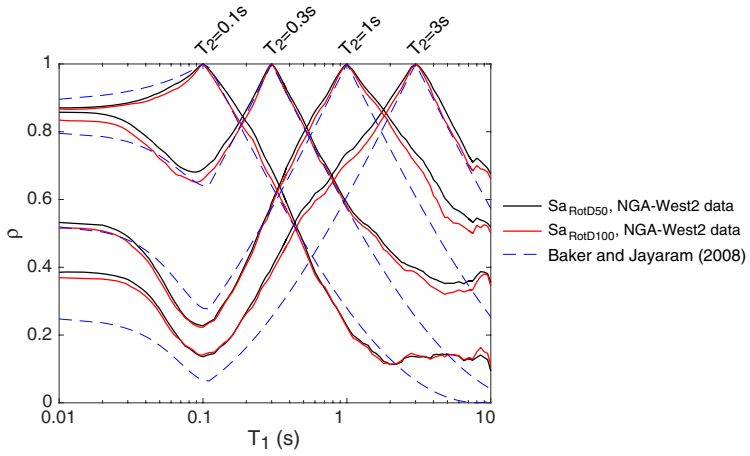

Figure 3. Correlation coefficients for $SA(T_1)$ and $SA(T_2)$, for four values of T_2, and for SA_{RotD50} and $SA_{RotD100}$ spectral acceleration definitions. Predicted correlations from Baker and Jayaram (2008) are superimposed for reference.

DEPENDENCE OF CORRELATIONS ON MAGNITUDE, DISTANCE AND V_{S30}

We next explore whether the above correlations show any dependence on M, R, or V_{S30}. Such an examination is important because it is conventionally assumed that the correlation coefficients are independent of these factors (and *Rup* and *Site* parameters, in general). We perform this evaluation by selecting subsets of the ground motion data from a given M, R, or V_{S30} range, and then computing correlations for that bin of data. We then vary the range, and evaluate potential variations in the associated correlation coefficients.

Figure 4 shows estimated spectral acceleration correlations for recordings with $R < 100$ km, and either $M > 6$ or $M < 4.5$, for several sets of periods. While the large-M and small-M correlations are in general agreement, there are some ranges (e.g., $T_1 < 0.1$ s and $T_2 = 1$ s) where the two appear to deviate.

To explore potential deviations more systematically, Figure 5 shows estimated correlations for pairs of *IM* values, as the M, R, or V_{S30} values of the input ground motions are varied. The left column shows correlations for four pairs of *SA* values (chosen to cover a range of periods and a range of correlation levels), and the right column shows correlations of four *SA* values with 5–75% significant duration. The top row uses ground motions with $R < 100$ km and binned magnitudes ($+/-$ 0.5 units around the target value); because duration values were only available for the large magnitude ground motions in the database, the range of considered magnitude values in Figure 5b is smaller than that in Figure 5a. The second row uses ground motions with $M > 5$ and binned distances ($+/-$ 10 km around the target value). The third row uses ground motions with $M > 5$, $R < 100$ km, and binned V_{S30} values ($+/-$ 100 m/s around the target). For all eight pairs of *IM* values shown in this figure, there is no apparent trend for the correlations to vary with M, R, or V_{S30}. Evaluations of additional *IM* pairs in this manner also revealed no systematic trends.

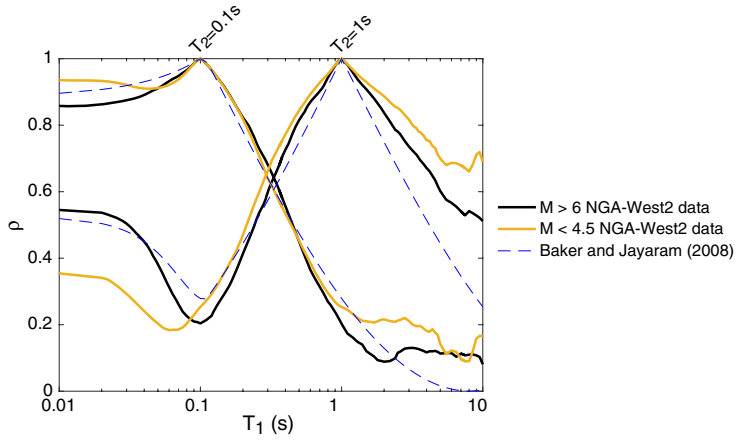

Figure 4. Correlation coefficients for $SA(0.1\,\mathrm{s})$ and $SA(1\,\mathrm{s})$, versus SA at other periods. Results are shown for ground motions from $M > 6$ or $M < 4.5$ earthquakes, and the Baker Jayaram (2008) predictive model for comparison.

These results are consistent with the finding of Carlton and Abrahamson (2014) that "any variation in correlation coefficients comes from spectral shape rather than tectonic region, and that generic correlation models are robust" (p. 511). Carlton and Abrahamson (2014) do find that correlation coefficients at short periods change somewhat depending upon the period at which the peak of the acceleration response spectrum occurs, and suggest that this effect could influence correlations for hard-rock sites with increased high frequency content; they propose a straightforward correlation modification procedure for such cases (the ground motion database used here does not have a sufficient number of true hard rock sites to further evaluate that conclusion using the approach of this paper).

The results of Figure 5 contradict Azarbakht et al. (2014), who claimed to find differences in correlation for some bins of data from specific magnitude and distance ranges. Given the lack of systematic trends in their reported correlations, and the lack of physical explanation for their reported differences, we suspect that the apparent differences they report are an artifact of small-sample variability and lack of mixed-effects treatment when computing correlation coefficients using data from a small number of earthquakes.

POSITIVE DEFINITE AGGREGATE CORRELATION MODEL

Because correlation estimates use differing ground motion data for each pair of IMs, and because the reference predictive models used above involve parametric approximations, the resulting correlation matrices for the collection of IMs are typically not positive definite, preventing some intended uses of the correlation matrix (such as in simulating realizations of IMs). For such applications, the approach of Qi and Sun (2006) is suggested to find the nearest positive-definite correlation matrix—a matrix that is practically equivalent to the original matrix in numerical values. Both raw correlation matrices and positive definite matrices for the discussed IM values are provided in an online Appendix.

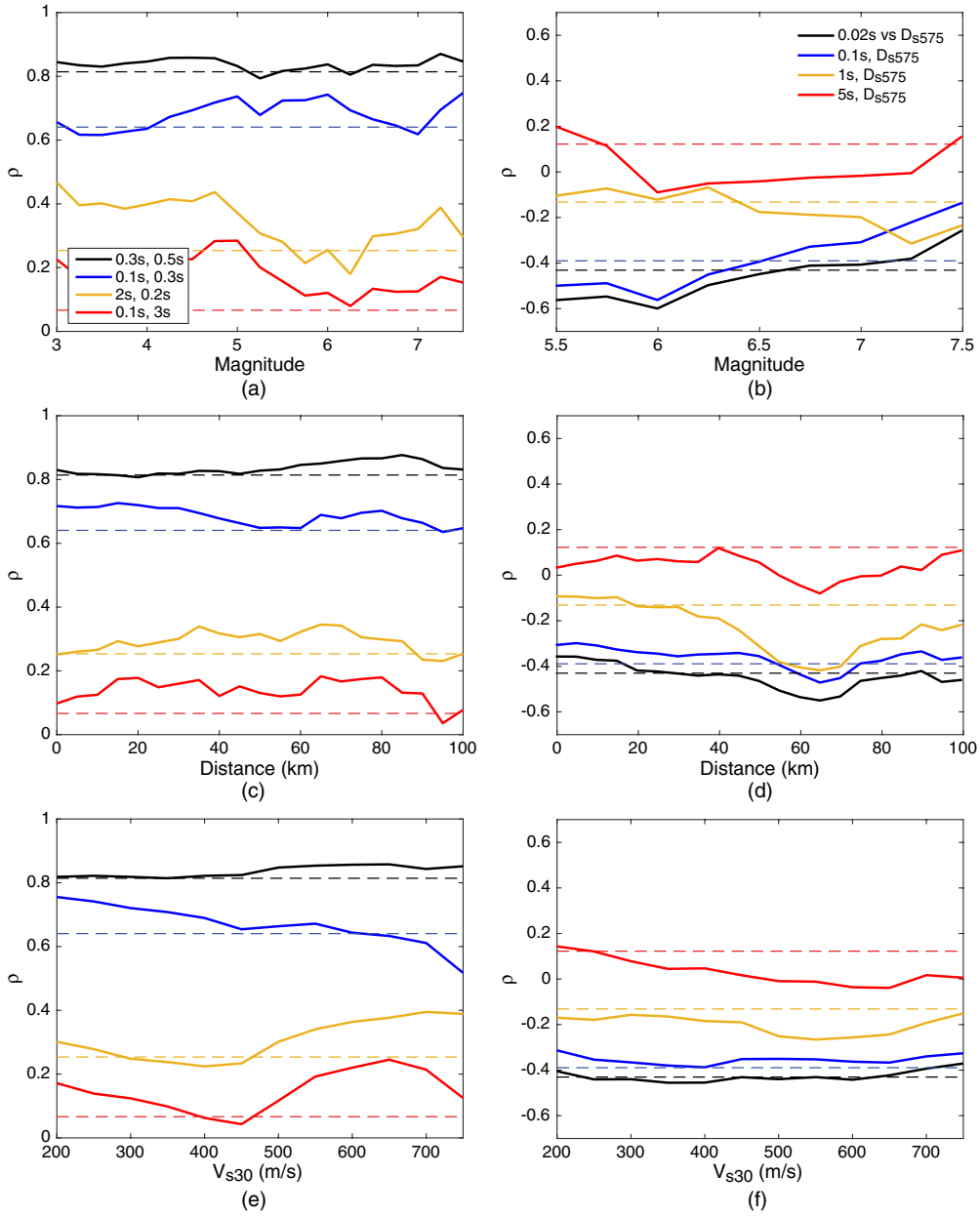

Figure 5. Correlation coefficients for pairs of *IM* values, as estimated from ground motions with a narrow range of M, R, or V_{S30}. *SA* correlations are shown on the left, and *SA*-versus-duration correlations on the right. Solid lines are estimates from data, and dashed lines are correlations from reference predictive models (Baker and Jayaram 2008 in the left column and Bradley 2011a in the right column).

EXAMPLE

The most frequent application for these correlation coefficients is in computation of a Conditional Spectrum. We note that the mean and standard deviation of log SA values are computed with the following equations:

$$\mu_{\ln SA(T_i)|\ln SA(T^*)} = \mu_{\ln SA}(Rup,Site,T_i) + \rho(T_i,T^*)\varepsilon(T^*)\sigma_{\ln Sa}(T_i) \tag{3}$$

$$\sigma_{\ln SA(T_i)|\ln SA(T^*)} = \sigma_{\ln SA}(T_i)\sqrt{1-\rho^2(T_i,T^*)} \tag{4}$$

where $\mu_{\ln SA(T_i)|\ln SA(T^*)}$ and $\sigma_{\ln SA(T_i)|\ln SA(T^*)}$ denote the mean and standard deviation, respectively, of ln SA, conditioned on ln SA at conditioning period T^* having a specified amplitude. The $\mu_{\ln SA}$ and $\sigma_{\ln SA}$ terms are the mean and standard deviation, respectively, from a GMM as discussed in Equation 1. The $\rho(T_i,T^*)$ term is the correlation coefficient between ln $SA(T^*)$ and ln $SA(T_i)$—the focus of the above analysis. The $\varepsilon(T^*)$ term is a variate defined by the following equation:

$$\varepsilon(T^*) = \frac{\ln SA(T^*) - \mu_{\ln SA}(Rup,Site,T^*)}{\sigma_{\ln SA}(T^*)} \tag{5}$$

These equations are provided to illustrate that Conditional Spectra depend upon both the $\rho(T_i,T^*)$ that is the focus here, as well as means and standard deviations from a reference GMM. And while $\rho(T_i,T^*)$ values sometimes vary by 0.1 or more between data sets or between models, this variation should be considered within the context of the effects of GMM choice.

To illustrate, Figure 6 shows the conditional mean and $+/-2$ standard deviations (of ln SA), using several permutations of input models. Calculations are shown for a vertical strike-slip fault with $M = 7.5$, $R = 20$ km, and $V_{S30} = 500$ m/s. Results are shown conditional on $SA(1\,\text{s}) = 0.75$ g, an amplitude that produces $\varepsilon(T^*) = 1.5$ using the Chiou and Youngs GMM.

Figure 6a shows results obtained using the Chiou and Youngs (2014) GMM and two estimates of correlations: the estimate from the data considered in this study, and the prediction from Baker and Jayaram (2008). Figure 6b shows results obtained using the Chiou and Youngs (2014) and the Boore et al. (2014) GMMs, with correlations estimated in this study. Qualitatively, we see that the Figure 6b results vary more substantially at many periods than the Figure 6a results.

To be more specific, let us consider results at a period of 10 s (i.e., $T^* = 1$ s, $T_i = 10$ s). This was seen in Figure 1c to be a case with a large difference between data and predictive model correlations: $\rho = 0.52$ from the data considered in this study versus $\rho = 0.25$ from the Baker and Jayaram (2008) model. The SA values at 10 s associated with conditional means in Figure 6a (0.017 g versus 0.013 g) differ by approximately 30%, versus the factor-of-two variation in $SA(10\,\text{s})$ values in Figure 6b (0.017 g versus 0.036 g).

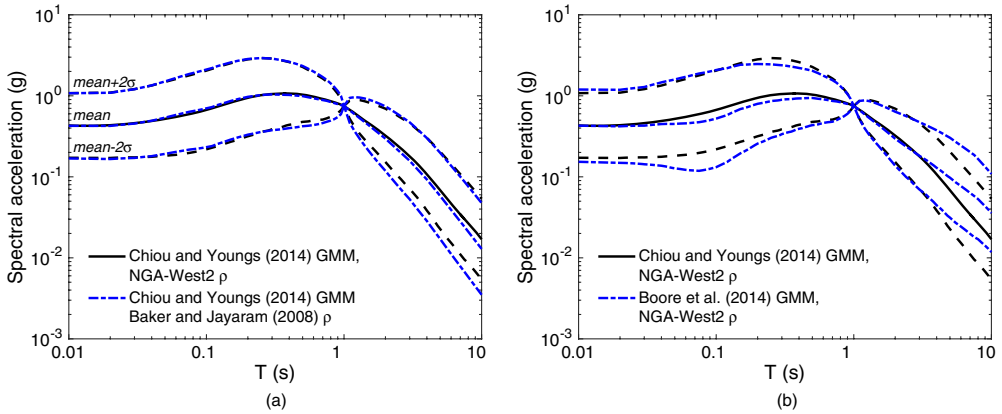

Figure 6. Conditional spectra for an $M = 7.5$, $R = 20$ km ground motion with $V_{S30} = 500$ m/s, conditioned on $SA(1\,\text{s}) = 0.75$ g. (a) Using the Chiou and Youngs (2014) GMM, and two correlation models. (b) Using two reference GMMs and the correlations from this study.

We note that the differences in spectral results at 10 s are the most extreme (both with regard to GMM predictions and correlation predictions), as would be expected due to the limited amount of usable ground motion data available at long periods. Results at other periods show lesser differences (and sometimes almost no difference among cases). While these variations are dependent upon many factors such as the GMMs, *Rup*, *Site*, and *IM*s considered, we expect that in most cases the differences in correlations among models will have a lesser effect on target spectra than the differences in means and standard deviations from the adopted GMMs.

CONCLUSIONS

We evaluated *IM* correlations using the new NGA-West2 ground motion database. The correlations were largely consistent with prior correlations estimated from alternative ground motion databases, confirming the understanding that these correlations are largely independent of the reference ground motion model and ground motion database. We recommend using the new correlation values computed here and provided in the electronic supplement, though previously published predictive models for these correlations are also likely suitable for most applications. While there are some differences in the results presented here relative to the predictive models they supersede, it is expected (and demonstrated via one anecdotal example) that the observed differences will generally not have a substantive impact on engineering calculations.

We computed spectral acceleration correlations for the SA_{RotD50} and $SA_{RotD100}$ definitions of response spectra for multicomponent ground motions (the two most common definitions), and found that the two are essentially identical. This is not surprising, given that SA_{RotD50} and $SA_{RotD100}$ values for a given ground motion tend to be similar (compared to their variability relative to GMM predictions). This indicates that existing correlation models, which were

typically developed for for SA_{RotD50} or some similar definition, can be adopted for calculation procedures using $SA_{RotD100}$ response spectra.

Finally, utilizing the wide range of earthquakes represented in the NGA-West2 database, we studied the dependence of *IM* correlations on magnitude, distance and V_{S30}. We were unable to detect any systematic variation of *IM* correlations with any of these parameters, lending further support to the typical assumption that *IM* correlations are independent of these parameters.

ACKNOWLEDGMENTS

This work was supported in part by the State of California through the Transportation Systems Research Program of the Pacific Earthquake Engineering Research Center (PEER). We thank Yousef Bozorgnia for providing RotD100 spectral data for the NGA-West2 database and Kioumars Afshari for providing code implementing his GMM. We thank Peter Stafford for helpful comments on the paper, and Katsuichiro Goda and Gian Paolo Cimellaro for their comments on the comparison of correlations among various models.

APPENDIX

Empirically estimated correlation coefficients from this study, as well as predicted correlations from prior predictive models, are provided as comma-separated value (CSV) files; versions of these correlations with minor modifications to make them collectively positive definite are also provided. Additionally, the raw data and Matlab source code used to perform the above analysis and produce the above figures is available at https://github.com/bakerjw/NGAW2_correlations.

REFERENCES

Abrahamson, N. A., Silva, W. J., and Kamai, R., 2014. Summary of the ASK14 ground motion relation for active crustal regions, *Earthquake Spectra* **30**, 1025–1055.

Afshari, K., and Stewart, J. P., 2016. Physically parameterized prediction equations for significant duration in active crustal regions, *Earthquake Spectra* **32**, 2057–2081.

Akkar, S., Sandikkaya, M. A., and Ay, B. Ö., 2014. Compatible ground-motion prediction equations for damping scaling factors and vertical-to-horizontal spectral amplitude ratios for the broader Europe region, *Bull Earthq Eng* **12**, 517–547.

Al Atik, L., 2011. Correlation of spectral acceleration values for subduction and crustal models, in *COSMOS Technical Session*, Emeryville, CA.

Al Atik, L., Abrahamson, N., Bommer, J. J., Scherbaum, F., Cotton, F., and Kuehn, N., 2010. The variability of ground-motion prediction models and its components, *Seismol Res Lett* **81**, 794–801.

American Society of Civil Engineers (ASCE), 2016. *Minimum Design Loads for Buildings and Other Structures*, ASCE 7-16, Reston, VA.

Ancheta, T. D., Darragh, R. B., Stewart, J. P., Seyhan, E., Silva, W. J., Chiou, B. S.-J., Wooddell, K. E., Graves, R. W., Kottke, A. R., Boore, D. M., Kishida, T., and Donahue, J. L., 2014. NGA-West2 database, *Earthquake Spectra* **30**, 989–1005.

Azarbakht, A., Mousavi, M., Nourizadeh, M., and Shahri, M., 2014. Dependence of correlations between spectral accelerations at multiple periods on magnitude and distance, *Earthq Eng Struct Dyn* **43**, 1193–1204.

Baker, J. W., and Cornell, C. A., 2005. A vector-valued ground motion intensity measure consisting of spectral acceleration and epsilon, *Earthq Eng Struct Dyn* **34**, 1193–1217.

Baker, J. W., and Jayaram, N., 2008. Correlation of spectral acceleration values from NGA ground motion models, *Earthquake Spectra* **24**, 299–317.

Boore, D. M., 2010. Orientation-independent, nongeometric-mean measures of seismic intensity from two horizontal components of motion, *Bull Seismol Soc Am* **100**, 1830–1835.

Boore, D. M., Stewart, J. P., Seyhan, E., and Atkinson, G. M., 2014. NGA-West2 equations for predicting PGA, PGV, and 5% damped PSA for shallow crustal earthquakes, *Earthquake Spectra* **30**, 1057–1085.

Bradley, B. A., 2010. A generalized conditional intensity measure approach and holistic ground-motion selection, *Earthq Eng Struct Dyn* **39**, 1321–1342.

Bradley, B. A., 2011a. Correlation of significant duration with amplitude and cumulative intensity measures and its use in ground motion selection, *J Earthq Eng* **15**, 809–832.

Bradley, B. A., 2011b. Empirical correlation of PGA, spectral accelerations and spectrum intensities from active shallow crustal earthquakes, *Earthq Eng Struct Dyn* **40**, 1707–1721.

Bradley, B. A., 2012. Empirical correlations between peak ground velocity and spectrum-based intensity measures, *Earthq Spectra* **28**, 17–35.

Campbell, K. W., and Bozorgnia, Y., 2014. NGA-West2 ground motion model for the average horizontal components of PGA, PGV, and 5% damped linear acceleration response spectra, *Earthquake Spectra* **30**, 1087–1115.

Carlton, B., and Abrahamson, N., 2014. Issues and approaches for implementing conditional mean spectra in practice, *Bull Seismol Soc Am* **104**, 503–512.

Chiou, B. S.-J., and Youngs, R. R., 2014. Update of the Chiou and Youngs NGA model for the average horizontal component of peak ground motion and response spectra, *Earthquake Spectra* **30**, 1117–1153.

Cimellaro, G. P., 2013. Correlation in spectral accelerations for earthquakes in Europe, *Earthq Eng Struct Dyn* **42**, 623–633.

Goda, K., and Atkinson, G. M., 2009. Probabilistic characterization of spatially correlated response spectra for earthquakes in Japan, *Bull Seismol Soc Am* **99**, 3003–3020.

Jayaram, N., and Baker, J. W., 2010. Considering spatial correlation in mixed-effects regression, and impact on ground-motion models, *Bull Seismol Soc Am* **100**, 3295–3303.

Qi, H., and Sun, D., 2006. A quadratically convergent Newton method for computing the nearest correlation matrix, *SIAM J Matrix Anal Appl* **28**, 360–385.

Shahi, S. K., and Baker, J. W., 2014. NGA-West2 models for ground-motion directionality, *Earthquake Spectra* **30**, 1285–1300.

Zimmerman, R. B., Baker, J. W., Hooper, J. D., Bono, S., Haselton, C. B., Engel, A., Hamburger, R. O., Celikbas, A., and Jalalian, A., 2017. Response history analysis for the design of new buildings in the NEHRP Provisions and ASCE/SEI 7 Standard: Part III - example applications illustrating the recommended methodology, *Earthquake Spectra*, in press, doi: http://dx.doi.org/10.1193/061814EQS087M.

(Received 7 June 2016; accepted 18 August 2016)